Immersed Boundary Models of Biofilm Spread

Ana Carpio and Rafael González-Albaladejo

Abstract We propose an immerse boundary approach for the dynamics of active contours in flows. When the active contours represent bacterial boundaries, we couple this system with dynamic energy budget models of cell metabolism for the evolution of the cell boundaries, informed by reaction-diffusion systems for the relevant concentration fields. Numerical simulations illustrate the evolution of incipient biofilms formed by clusters of spherical bacteria in two dimensions.

1 Introduction

Immersed boundary (IB) methods [13, 14] provide efficient tools to handle fluid/structure interactions in many applications. Our goal here is to adapt them to describe the behavior of cellular systems such as bacterial biofilms, in which the structures are cell membranes. Biofilms are bacterial aggregates encased in a self-produced polymeric matrix which grow on moist surfaces [6] and are responsible for most hospital acquired infections [8]. Many models have been developed to study their behavior, focusing on different aspects: continuous models [17], agent based descriptions [7, 10, 11, 18, 20] and hybrid models combining both [2, 16]. Immersed boundary methods have already been used to study finger deformation [20], viscoelastic behavior [19] and attachment of bacteria [4] in flows. Active cellular contours have been addressed by removing the incompressibility constraint and including inner sources [12]. Applications to multicellular tissues

A. Carpio
Universidad Complutense de Madrid, Madrid, Spain
e-mail: ana_carpio@mat.ucm.es

R. González-Albaladejo (✉)
Universidad Complutense de Madrid, Madrid, Spain

Instituto Gregorio Millán, Universidad Carlos III de Madrid, Madrid, Spain
e-mail: rafael09@ucm.es

M. Ehrhardt, M. Günther (eds.), *Progress in Industrial Mathematics at ECMI 2021*,
The European Consortium for Mathematics in Industry 39,
https://doi.org/10.1007/978-3-031-11818-0_8

[5, 15] consider closely packed deformable contours attached to each other [5, 15]. However, bacterial biofilms are formed by rigid shapes which remain at a certain distance. When biofilms grow in flows, we usually have scattering bacteria in large polymer fractions. Instead, we consider here incipient biofilms spreading on surfaces, in which the volume fraction of polymeric matrix keeping cells together is small [17]. We propose a computational model that combines an IB description of cellular arrangements and mechanical interactions with a dynamic energy budget (DEB) representation of bacterial activity and chemical processes. Simple tests on clusters of spherical bacteria illustrate its potential to investigate cell arrangements and interaction with flows.

2 Immerse Boundary Model for Active Boundaries

Immersed boundary models are usually formulated for 'inert' boundaries whose shape changes as a result of the interaction with the fluid, keeping a fixed size. Cells are 'active' boundaries, whose size and number changes. Let us explain how this affects the standard IB equations. Given a region Ω and a boundary Γ immersed in it, the fluid-structure interaction is described by the incompressible Navier-Stokes equations set in Ω [13, 14]:

$$\frac{\partial \mathbf{u}}{\partial t} + \mathbf{u} \cdot \nabla \mathbf{u} = \nu \Delta \mathbf{u} - \frac{1}{\rho} \nabla p + \frac{1}{\rho} \mathbf{f} - \frac{\alpha}{\rho} \mathbf{u}, \quad \text{div}(\mathbf{u}) = 0, \tag{1}$$

where $\mathbf{u}(\mathbf{x}, t)$, $p(\mathbf{x}, t)$ and $\mathbf{f}(\mathbf{x}, t)$ are the fluid velocity, fluid pressure and external force density. The parameters ρ, $\nu = \mu\rho$ and α denote the fluid density, kinematic viscosity and friction coefficient, respectively. We enforce periodic boundary conditions for the fluid, which allows to use fast solvers based on fast Fourier transforms [13, 14], and place Γ far from the boundaries to allow for free growth while reducing boundary effects. The force $\mathbf{f}(\mathbf{x}, t)$ created by Γ on the fluid is

$$\mathbf{f}(\mathbf{x}, t) = \int_{\Gamma} \mathbf{F}(\mathbf{q}, t) \delta(\mathbf{x} - \mathbf{X}(\mathbf{q}, t))\, d\mathbf{q}. \tag{2}$$

In practice, the delta function δ is replaced for computational purposes with adequate regularizations [13, 14]. $\mathbf{X}(\mathbf{q}, t)$ is the parametrization of Γ, and $\mathbf{F}(\mathbf{q}, t)$ is the force density on it. The integration parameters $\mathbf{q}$ represent angles. When several cells are present, we work with several parametrizations $\mathbf{X}_1, \ldots, \mathbf{X}_N$.

The evolution equation for Γ follows correcting the no-slip condition

$$\frac{\partial \mathbf{X}}{\partial t} = \int_{\Omega} \mathbf{u}(\mathbf{x}, t) \delta(\mathbf{x} - \mathbf{X}(\mathbf{q}, t))\, d\mathbf{x} + \lambda \big((\mathbf{F}_g \cdot \mathbf{n}) \mathbf{n} + \mathbf{F}_{ext} \big), \quad \lambda > 0, \tag{3}$$

with the contribution of growth $\mathbf{F}_g$ and external forces $\mathbf{F}_{ext}$. In practice, $\mathbf{F} = \mathbf{F}_e + \mathbf{F}_g + \mathbf{F}_{ext}$. Elastic forces $\mathbf{F}_e$ within the IB are tangent to the outer normal $\mathbf{F}_e \cdot \mathbf{n} = 0$. In two dimensions, and assuming the boundaries are formed by springs parametrized by the angle θ, $\mathbf{F}_e = \frac{\partial}{\partial\theta}\left(K\frac{\partial \mathbf{X}}{\partial\theta}\right)$, for an elastic constant K [13, 14]. Standard IB approaches set $\mathbf{F}_g = \mathbf{F}_{ext} = 0$ and $\alpha = 0$. Here, the friction parameter $\alpha > 0$ represents the effect of the polymeric matrix enveloping bacteria and hindering their motion. The growth forces are included since they modify the size of Γ. We set them proportional to $\frac{dR}{dt}\mathbf{n}$, being R the radius of each bacterium, see [3] for more details. In our case, $\mathbf{F}_{ext} = \mathbf{F}_i$ are interaction forces between bacteria, moving them as blocks. For spherical bacteria, we set $\mathbf{F}_i = \sum_{j=1}^{N} \mathbf{F}_{i,j}\delta_j$ with

$$\mathbf{F}_{i,j} = \begin{cases} \displaystyle\sum_{n=1,n\neq j}^{N} \frac{\sigma}{d_{min}}\mathbf{n}_{\mathrm{cm},n,j} & \text{if } d_{j,n} \leq d_{min}, \\ \displaystyle\sum_{n=1,n\neq j}^{N} \frac{\sigma\left(1+\tanh\left(\frac{s_p - d_{j,n}}{v_p}\right)\right)}{2d_{j,n}}\mathbf{n}_{\mathrm{cm},n,j} & \text{if } d_{j,n} > d_{min}, \end{cases} \tag{4}$$

where σ is a repulsion parameter, $\mathbf{n}_{\mathrm{cm},n,j} = \frac{\mathbf{X}_{c,j} - \mathbf{X}_{c,n}}{\|\mathbf{X}_{c,j} - \mathbf{X}_{c,n}\|}$ the unit vector that joins the centers of mass, and $d_{j,n}$ the distance between them. Here, δ_j equals 1 on the boundary $\mathbf{X}_j$ and vanishes on the rest. s_p controls at what distance the force begins to act and v_p its growth if the distance continues to decrease, see [3]. This force is easy to adjust and extend to rod-like shapes by tuning parameters [3], as opposed to the forces employed in [7]. Resorting to Morse potentials would be too expensive, whereas Lennard-Jones potentials seem too strong.

3 Dynamic Energy Budget Model for Cell Metabolism

The growth dynamics of the boundaries representing bacterial membranes is governed by bacterial metabolism. We use a Dynamic energy budget (DEB) [1, 9] model for each cell, informed by a set of relevant concentration fields.

Given N bacteria, their energy e_j and volume V_j, $j = 1, \ldots, N$, are governed by

$$\frac{de_j}{dt} = \nu'\left(\frac{S}{S+K_S} - e_j\right), \quad \frac{dV_j}{dt} = \left(r_j\frac{a_j}{a_M} - h_j\right)V_j, \qquad r_j = \left(\frac{\nu' e_j - mg}{e_j + g}\right)^{+}, \tag{5}$$

where $\nu' = \nu e^{-\gamma\varepsilon}$, ν is the energy conductance, γ the environmental degradation coefficient, K_S a half-saturation coefficient, m the maintenance rate, g the investment ratio and a_M the target acclimation energy. The symbol $^+$ stands for 'positive part'. The factor r_j denotes the bacterial production rate. For 2D spherical bacteria

$V_j = \pi R_j^2$, and (5) implies

$$2\frac{dR_j}{dt} = \left(r_j \frac{a_j}{a_M} - h_j\right) R_j. \tag{6}$$

The aging q_j and hazard h_j variables represent damage on the cell, while a_j stands for acclimation, governed by

$$\frac{dq_j}{dt} = e_j(s_G \rho_x \frac{V_j}{V_T} q_j + h_a)(\nu - r_j) - (r_j + r_{e,j})q_j, \quad \frac{dh_j}{dt} = q_j - (r_j + r_{e,j})h_j, \tag{7}$$

$$\frac{dp_j}{dt} = -h_j p_j, \quad \frac{da_j}{dt} = (r_j + r_{e,j})\left(1 - \frac{a_j}{a_M}\right)^+, \tag{8}$$

where ρ_x is the cell density, h_a the Weibull aging acceleration, s_G a multiplicative stress coefficient. Here, p_j is the probability of survival at time t. The factor $r_{e,j} = kr_j + k'$, for $k, k' > 0$ when the cell is and polymer (EPS) producer, otherwise it vanishes. The produced EPS is then $\frac{dV_{e,j}}{dt} = r_{e,j} V_j$. A fraction $\eta \in (0, 1)$ diffuses creating a concentration of monomers C_e, while the rest sticks to the bacteria. The limiting substrate concentration S and environmental degradation ε satisfy

$$\frac{dS}{dt} = -\nu' \frac{S}{S + K_S} \rho_x \sum_j \frac{V_j}{V_T} \delta_j + d_s \Delta S - \mathbf{u} \cdot \nabla S, \tag{9}$$

$$\frac{dC_e}{dt} = \eta \rho_x \sum_j r_{e,j} \frac{V_j}{V_T} \delta_j + d_e \Delta C_e - \mathbf{u} \cdot \nabla C_e, \tag{10}$$

$$\frac{d\varepsilon}{dt} = \nu_\varepsilon \rho_x \sum_j (r_j + \nu_m m) \frac{V_j}{V_T} \delta_j + d_\varepsilon \Delta \varepsilon - \mathbf{u} \cdot \nabla \varepsilon, \tag{11}$$

where ν_m is the maintenance respiratory coefficient, ν_ε is the environmental degradation coefficient and d_s, d_e, d_ε diffusion coefficients. Here V_T is a reference volume and $\delta_j = 1$ at cell j, it vanishes otherwise. We enforce no flux boundary conditions, except for S, which remains constant at the borders.

We couple the system of ordinary differential equations (5)–(7) and the reaction-diffusion equations (9)–(11) using a similar philosophy as that in IB models. We spread fields defined on bacteria using the cell volumes and rates as sources in equations (9)–(11). We interpolate global fields on the bacteria averaging values of S, ε in the region occupied by the cell. For each cell, the systems (5)–(7) are discretized order two Runge-Kutta schemes. The reaction-diffusion equations (9)–(11) are discretized by classical explicit finite difference schemes, first order in time and second order in space.

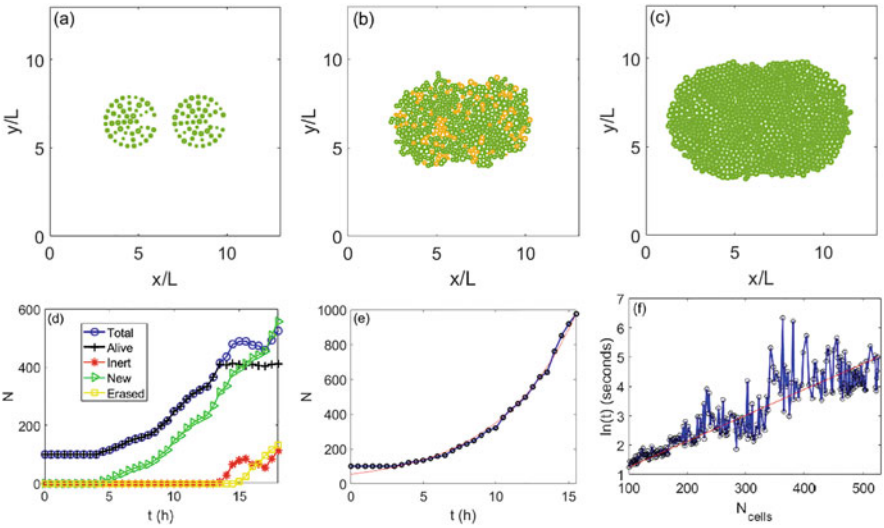

Fig. 1 (**a**) Initial configuration. Simulated configurations (**b**) after 18 hours with $h_0 = 0.4$ and (**c**) after 15 hours with $h_0 = 0$ (no death). While (**b**) has 412 live cells (green) and 113 dead cells (orange), (**c**) contains 920 live cells. Growth curve of cell types versus time (**d**) for simulation (**b**) and (**e**) for simulation (**c**). The red fit in (**e**) is $t \sim Ce^{\gamma N}$, where $C \sim 54.53$ and $\gamma \sim 0.1861$ [1/h], N being the number of cells. Panel (**f**) shows the times required to perform one computational step depending on the number of cells in simulation (**a**)–(**b**) (blue circles) compared to its exponential fit (red), $Ce^{\gamma t}$, where $C \sim 1.4421$ [s] and $\gamma \sim 0.0088$

4 Simulations of Biofilm Spread

For typical parameter values [1, 3], the IB and concentration submodels are quasistationary. Their solutions evolve as the immersed boundaries grow, shrink, divide or move due to interactions. We solve the DEB equations (5)–(7) in a time scale of hours, while updating the IB and concentration fields using time relaxation schemes to update the quasistationary fields. Results are displayed in Fig. 1. Cells $\mathbf{X}_j$ die when $1 - p_j > \frac{N_{init}}{N_a} + r\left(1 - \frac{N_{init}}{N_a}\right)$, N_a and N_{init} being the current and the initial number of bacteria while $r \in (0, 1)$ is a random number [3]. Cells divide in two when their size surpasses a critical value.

5 Conclusions and Perspectives

Modeling the behavior of cell aggregates such as bacterial biofilms confronts the difficulties of handling complicated interactions and geometries. We propose an immerse boundary approach with enhanced spatial resolution when compared to particle or cellular automata descriptions, since we can track individual deforma-

tions and fluid-structure interactions. This approach is computationally expensive if we aim to grow large clusters to see behaviors emanating at larger scales. However, High Performance Computing tools may help to overcome that burden. The present work focuses on spherical bacteria. Extensions to other shapes (rod-like, mixtures), geometries (interaction with barriers) and environments (inclusion of toxicants) can be envisaged [3]. In our current simulations the fluid flow has little relevance. Exploring interactions with the flow and its influence on the observed shapes [16] should be the subject of further work.

Acknowledgments Research partially supported by Spanish FEDER/MICINN-AEI grants MTM 2017-84446-C2-1-R and PID2020-112796RB-C21 (AC, RG), by fellowship PRE2018-083807 (RG), and by the MICINN 'Salvador de Madariaga" grant PRX18/00112 (AC). A.C. thanks C.S. Peskin for fruitful discussions and suggestions during a sabbatical stay at NYU.

References

1. B. Birnir, A. Carpio, E. Cebrián, P. Vidal, Dynamic energy budget approach to evaluate antibiotic effects on biofilms, Commun. Nonlinear Sci. Numer. Simulat. 54 (2002) 70–83.
2. A. Carpio, E. Cebrián, P. Vidal, Biofilms as poroelastic materials, Int. J. Non-Linear Mech. 109 (2019) 1–8.
3. A. Carpio, R. González-Albaladejo, Immersed boundary approach to biofilm spread on surfaces, Commun. Comput. Phys. 31 (1), 257–292, 2022.
4. R. Dillon, L. Fauci, A. Fogelson, D. Gaver, Modeling biofilm processes using the immersed boundary method, J. Comput. Phys. 129 (1996) 57–73.
5. R. Dillon, M. Owen, K. Painter, A single-cell-based model of multicellular growth using the immersed boundary method, In: Moving Interface Problems and Applications in Fluid Dynamics (pp. 1–16). (Contemporary Mathematics). American Mathematical Society, 2008.
6. H.C. Flemming, J. Wingender, The biofilm matrix, Nat. Rev. Microbiol. 8 (2010) 623–633.
7. M.A.A. Grant, B. Waclaw, R.J. Allen, P. Cicuta, The role of mechanical forces in the planar-to-bulk transition in growing *Escherichia coli* microcolonies, J. R. Soc. Interface 11 (2014) 20140400.
8. N. Høiby, T. Bjarnsholt, M. Givskov, S. Molin, O. Ciofu, Antibiotic resistance of bacterial biofilms, Int J Antimicrob Agents 35 (2010) 322–32.
9. T. Klanjscek, R.M. Nisbet, J.H. Priester, P.A. Holden, Modeling physiological processes that relate toxicant exposure and bacterial population dynamics, PLoS One 7(2) (2012) e26955.
10. L. A. Lardon, B. V. Merkey, S. Martins, et al, iDynoMiCS: next-generation individual-based modelling of biofilms, Environ. Microbiol. 13 (2011) 2416–34.
11. C. S. Laspidou, L. A. Spyrou, N. Aravas, B. E. Rittmann, Material modeling of biofilm mechanical properties, Math. Biosci. 251 (2014) 11–15.
12. Y. Li, A. Yun, J. Kim, An immersed boundary method for simulating a single axisymmetric cell growth and division, J. Math. Bio. 65 (2012) 653–675.
13. C.S. Peskin, D.M. McQueen, A general method for the computer simulation of biological systems interacting with fluids, Symposia of the Society for Experimental Biology 49 (1995) 265–76.
14. C.S. Peskin, The immersed boundary method, Acta Numerica 11 (2002) 479–517.
15. K.A. Rejniak, An immersed boundary framework for modelling the growth of individual cells: an application to the early tumour development, J. Theoret. Bio. 247 (2007) 186–204.
16. D. Rodriguez, B. Einarsson, A. Carpio, Biofilm growth on rugose surfaces, Phys. Rev. E 86 (2012) 061914.

17. A. Seminara, T.E. Angelini, J.N. Wilking, et al, Osmotic spreading of *Bacillus subtilis* biofilms driven by an extracellular matrix, Proc. Natl. Acad. Sci. USA 109 (2012) 1116–1121.
18. T. Storck, C. Picioreanu, B. Virdis, D.J. Batstone, Variable cell morphology approach for individual-based modeling of microbial communities, Biophys. J. 106 (2014) 2037–2048.
19. J.A. Stotsky, J.F. Hammond, L. Pavlovsky, et al, Variable viscosity and density biofilm simulations using an immersed boundary method, Part II: Experimental validation and the heterogeneous rheology-IBM, J. Comput. Phys. 317 (2016) 204–222.
20. R. Sudarsan, S. Ghosh, J.M. Stockie, H.J. Eberl, Simulating biofilm deformation and detachment with the immersed boundary method, Commun. Comput. Phys. 19 (2016) 682–732.